

Chiral hybrid manganese(II) halide clusters with circularly polarized luminescence as X-ray scintillators

Mengzhu Wang,^a Xiaoming Wang,^a Bintao Zhang,^a Feiyang Li,^a Haixing Meng,^a Shujuan Liu^{a,*} and Qiang Zhao^{a,b*}

^a State Key Laboratory of Organic Electronics and Information Displays & Jiangsu Key Laboratory for Biosensors, Institute of Advanced Materials (IAM) & Institute of Flexible Electronics (Future Technology), Nanjing University of Posts and Telecommunications (NUPT), 9 Wenyuan Road, Nanjing 210023, Jiangsu, P. R. China.

^b College of Electronic and Optical Engineering & College of Flexible Electronics (Future Technology), Jiangsu Province Engineering Research Center for Fabrication and Application of Special Optical Fiber Materials and Devices, Nanjing University of Posts and Telecommunications (NUPT), 9 Wenyuan Road, Nanjing 210023, Jiangsu, P. R. China.

Materials

All the raw materials, (R)-3-aminopyrrolidine dihydrochloride (R-C₄H₁₀N₂·2HCl) (98%), (S)-3-aminopyrrolidine dihydrochloride (S-C₄H₁₀N₂·2HCl) (98%), (R)-1,2-diaminopropane dihydrochloride (R-C₃H₁₀N₂·2HCl) (98%), (S)-1,2-diaminopropane dihydrochloride (S-C₃H₁₀N₂·2HCl) (98%) and manganese(II) chloride tetrahydrate (MnCl₂·4H₂O, 98%) were purchased from Leyan.com without further purification.

Synthesis of R1. MnCl₂·4H₂O (1.979 g) and (R)-3-aminopyrrolidine dihydrochloride (1.742 g) were added into the mixed solution of methanol (5 mL), and the solution was heated at 60 °C. The resulting solution was gradually cooled down to room temperature and evaporated in the atmosphere for 2 weeks. Bulk reddish crystals were obtained after vacuum drying with the yield of 96%. Anal. Calcd for C₂₄H₇₈N₁₂Cl₁₈Mn₃: C, 21.55%; H, 5.88%; N, 12.56%. Found: C, 21.40%; H, 6.01%; N, 12.41%.

Synthesis of S1. MnCl₂·4H₂O (1.979 g) and (S)-3-aminopyrrolidine dihydrochloride (1.742 g) were added into the mixed solution of methanol (5 mL), and the solution was heated at 60 °C. The resulting solution was gradually cooled down to room temperature

and evaporated in the atmosphere for 2 weeks. Bulk reddish crystals were obtained after vacuum drying with the yield of 94%. Anal. Calcd for $C_{24}H_{78}N_{12}Cl_{18}Mn_3$: C, 21.55%; H, 5.88%; N, 12.56%. Found: C, 21.28%; H, 5.98%; N, 12.32%.

Synthesis of R2. $MnCl_2 \cdot 4H_2O$ (1.979 g) and (R)-3-aminopyrrolidine dihydrochloride (1.742 g) were added into the mixed solution of methanol (5 mL), and the solution was heated at 60 °C. The resulting solution was gradually cooled down to room temperature and evaporated in the atmosphere for 2 weeks. Bulk reddish crystals were obtained after vacuum drying with the yield of 96%. Anal. Calcd for $C_{24}H_{78}N_{12}Cl_{18}Mn_3$: C, 21.55%; H, 5.88%; N, 12.56%. Found: C, 21.40%; H, 6.01%; N, 12.41%.

Synthesis of S2. $MnCl_2 \cdot 4H_2O$ (1.979 g) and (S)-3-aminopyrrolidine dihydrochloride (1.742 g) were added into the mixed solution of methanol (5 mL), and the solution was heated at 60 °C. The resulting solution was gradually cooled down to room temperature and evaporated in the atmosphere for 2 weeks. Bulk reddish crystals were obtained after vacuum drying with the yield of 94%. Anal. Calcd for $C_{24}H_{78}N_{12}Cl_{18}Mn_3$: C, 21.55%; H, 5.88%; N, 12.56%. Found: C, 21.28%; H, 5.98%; N, 12.32%.

Scintillation film preparation. R2 single crystals were ground to obtain crystal powders by using mortar and pestle. PMMA was added into toluene and ultrasonic treatment was performed until the solution turn transparent. A certain amount of R2 crystal powders were added into the above PMMA solution and a uniform paste suspension was formed after ultrasonic treatment. Then, the suspension was evenly drop-casted onto a 3 × 3 cm square glass slide and evaporated at room temperature for 24 h until the film was formed. All the above operations were performed in the fume hood.

Characterization

Single crystal suitable for Single-crystal X-ray diffraction (SCXRD) was selected through an optical microscope, the single crystal was put on top of the capillary and then placed on top of the goniometer head. At room temperature, using ω -2 θ scanning technology, the single crystal structure diffraction data was collected on the Bruker Smart Apex CCD Diffractometer with graphite-monochromatic Mo-K α ($\lambda = 0.71073$ Å). The single crystal structure was analyzed and refined by using the direct method

and the full small square method F^2 (SHELX-97 software). Powder X-ray diffraction was conducted on the X-ray diffractometer D8 Advance A25.

Thermogravimetric Analysis (TGA)

The TGA data was obtained through the NETZSCH STA-2500 at rate of 10 °C/min under pure nitrogen atmosphere (25-500 °C).

Optical Performance Measurements

Photoluminescence (PL) emission, excitation spectra and time-resolved PL decays were recorded by an Edinburgh FLS-980 spectrophotometer equipped with 450 W xenon lamp source and flash lamp, and the lifetime measurement range is 100 ps-10 s. The photoluminescence quantum yields were measured by Edinburgh FLS-980 with an integrating sphere. The circular dichroism (CD) spectra were measured on a Jasco J-1500 circular dichroism spectrometer. The circularly polarized luminescence (CPL) spectra were measured on a Jasco CPL-300 spectrophotometer.

Calculation of X-ray Attenuation Efficiency

In order to obtain the attenuation efficiency (AE) of X-ray, we can calculate it by the following formula:

$$AE(\%) = (1 - e^{-c(\epsilon)\rho d}) \times 100\%$$

The X-ray absorption coefficient (α) is defined as follows: $\alpha = c(\epsilon) \times \rho$, where $c(\epsilon)$ represents the photon cross-section function obtained from the National Institute of Standards and Technology (NIST) XCOM database, while ρ is the scintillator density, ϵ is the corresponding photon energy, and d represents the thickness of the scintillator. To calculate the relationship between the scintillator thickness and the X-ray attenuation efficiency, we used 22 keV (the mean and peak value of our X-ray tube) as the photon energy. In order to standardize and calibrate the light conversion efficiency of scintillators, a commercial LuAG:Ce scintillator was used as a reference standard. To ensure the preciseness of the experiment, our samples and LuAG:Ce were ground into fine powder and prepared into scintillator wafers with same diameter of 1.3 cm and same thickness of 100 μm . Furthermore, we placed our scintillator and the reference scintillator strictly in the same position, and measured their RL spectra under the same

conditions. Then, the corresponding photon counting results (PC measured) were obtained by integrating the RL spectra. The steady-state X-ray to visible light conversion efficiency is defined as the ratio of the number of emitted photons to the total absorbed X-ray energy. From this point of view, the emitted photons should be normalized to the same X-ray attenuation (100%) using the following equation:

$$PC_{normalized} = \frac{PC_{measured}}{AE(d)}$$

where AE(d) represents the X-ray attenuation (%) of the scintillator at a certain thickness. Finally, the light conversion efficiency of our scintillator (LYs) were calculated from the following equation:

$$LY_S = LY_{LuAG:Ce} \frac{PC_{normalized}(S)}{PC_{normalized}(LuAG:Ce)}$$

where LY LuAG:Ce in the formula is the known light yield of 24900 photons/MeV for LuAG:Ce, PC normalized (S) and PC normalized (LuAG:Ce) represent the photon counts of our scintillator and LuAG:Ce after normalizing to the corresponding X-ray attenuation, respectively.

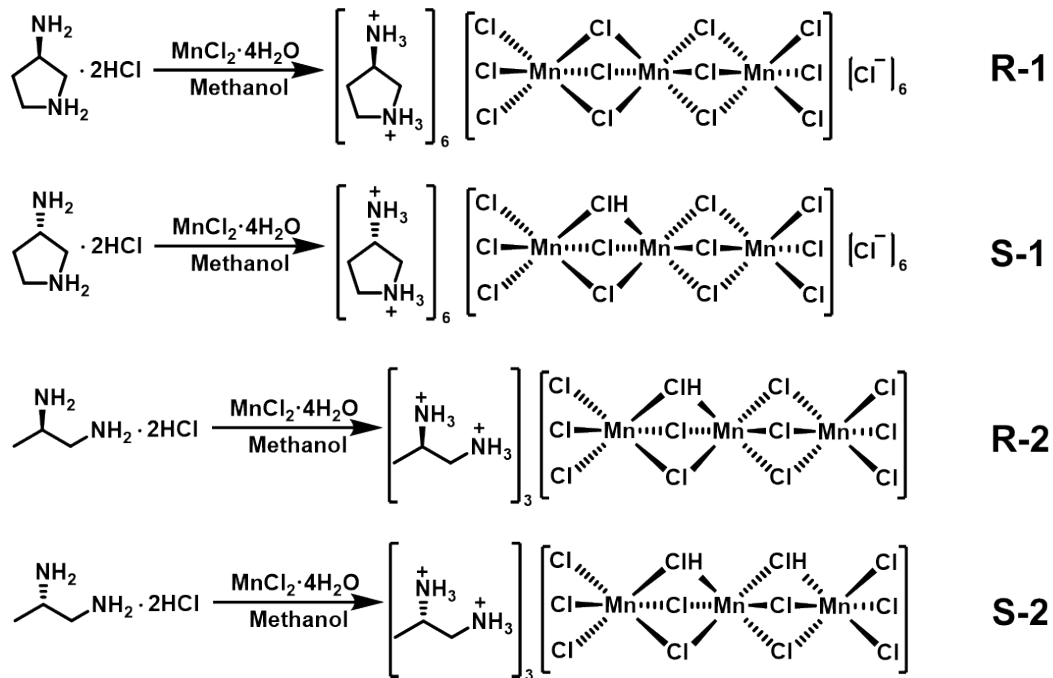


Fig. S1. Synthetic routes of halides clusters R/S-1 and R/S-2.

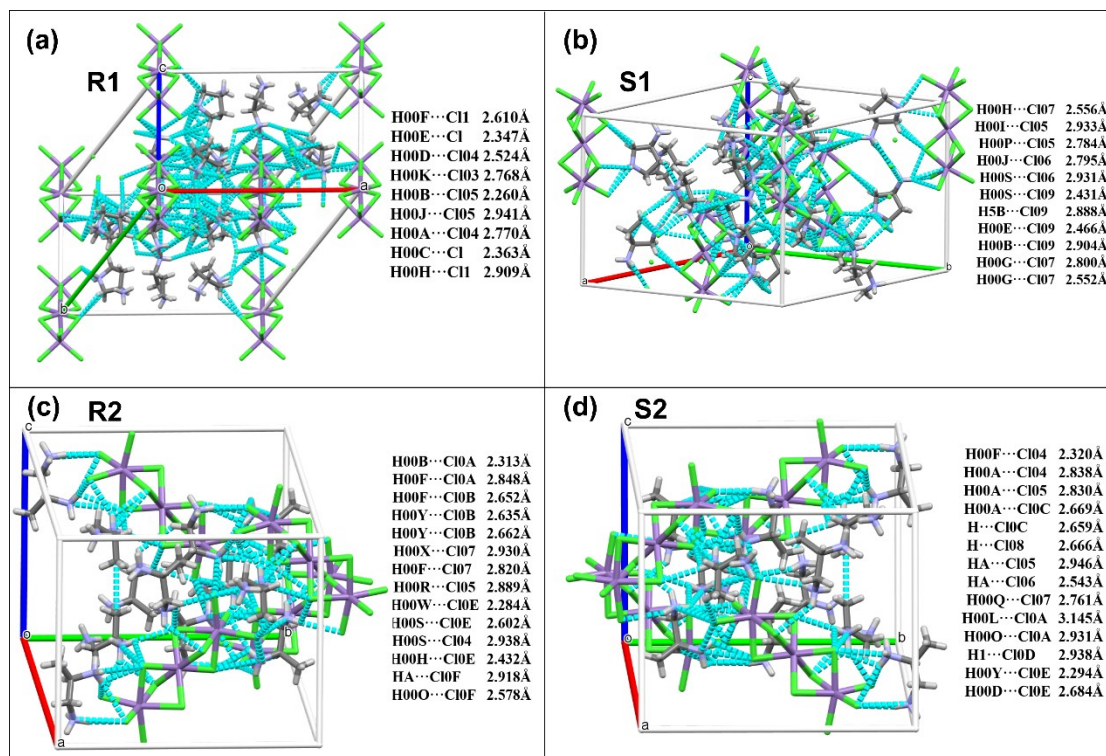


Fig. S2. The intramolecular interactions of halides clusters R/S-1 and R/S-2.

Table S1. Crystal data and structure refinement

	R-1	S-1	R-2	S-2
CCDC number	2219583	2219584	2219585	2219586
Empirical Formula	$C_{24}H_{72}Cl_{18}Mn_3N_{12}$	$C_{24}H_{72}Cl_{18}Mn_3N_{12}$	$C_9H_{36}Cl_{12}Mn_3N_6$	$C_9H_{36}Cl_{12}Mn_3N_6$
Formula weight	1331.85	1331.85	818.66	818.66
Temperature (K)	293	294.37	295.87	296.41
Crystal system	triclinic	trigonal	monoclinic	monoclinic
Space group	R32	R3	C2	C2
<i>a</i> (Å)	17.9444(12)	17.904(3)	15.654(4)	15.730(4)
<i>b</i> (Å)	17.9444(12)	17.904(3)	16.063(4)	16.116(4)
<i>c</i> (Å)	14.7348(9)	14.724(2)	12.743(3)	12.765(3)
α (°)	90	90	90	90

β (°)	90	90	108.103(5)	108.218(7)
γ (°)	120	120	90	90
Volume (Å ³)	4109.0(6)	4087.6(13)	3045.6(12)	3073.6(14)
Z	3	3	4	4
ρ_{calc} (g/cm ³)	1.615	1.623	1.785	1.769
F (000)	2043.0	2043.0	1644.0	1644.0
μ (mm ⁻¹)	1.593	1.601	2.290	2.270
Reflections collected	18419	12046	19767	18973
Goodness-of-fit on F^2	1.032	1.046	1.021	1.017
Final R indexes	R1 = 0.0376,	R1 = 0.0337,	R1= 0.0399,	R1 = 0.0460,
[$I > 2\sigma(I)$]	wR2 = 0.1009	wR2 = 0.0682	wR2=0.0996	wR2 = 0.1080
Final R indexes	R1=0.0538,	R1 = 0.0573,	R1= 0.0572,	R1 = 0.0758,
[all data]	wR2=0.1098	wR2 = 0.0753	wR2=0.1074	wR2 = 0.1201

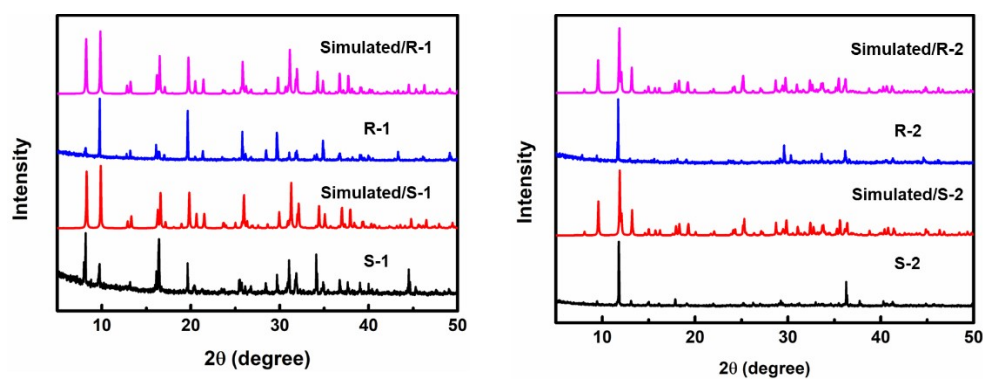


Fig. S3. The experimental powder XRD spectra of R/S-1 and R/S-2 compared with the simulated data from the single crystal structures.

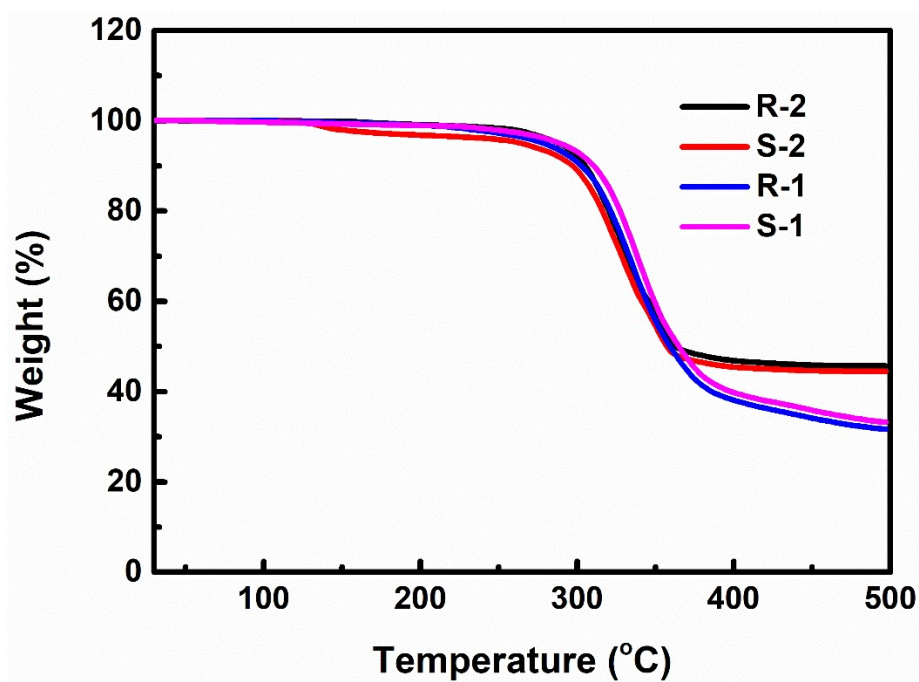


Fig. S4. TGA curves of R/S-1 and R/S-2.

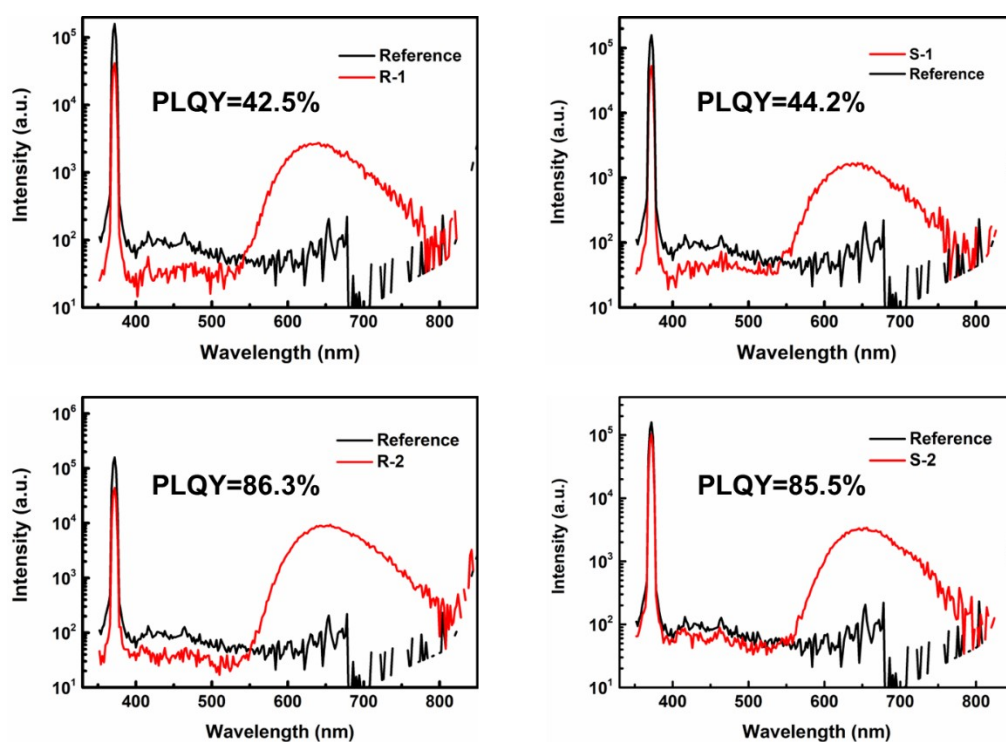


Fig. S5. The PLQY spectra of R/S-1 and R/S-2.

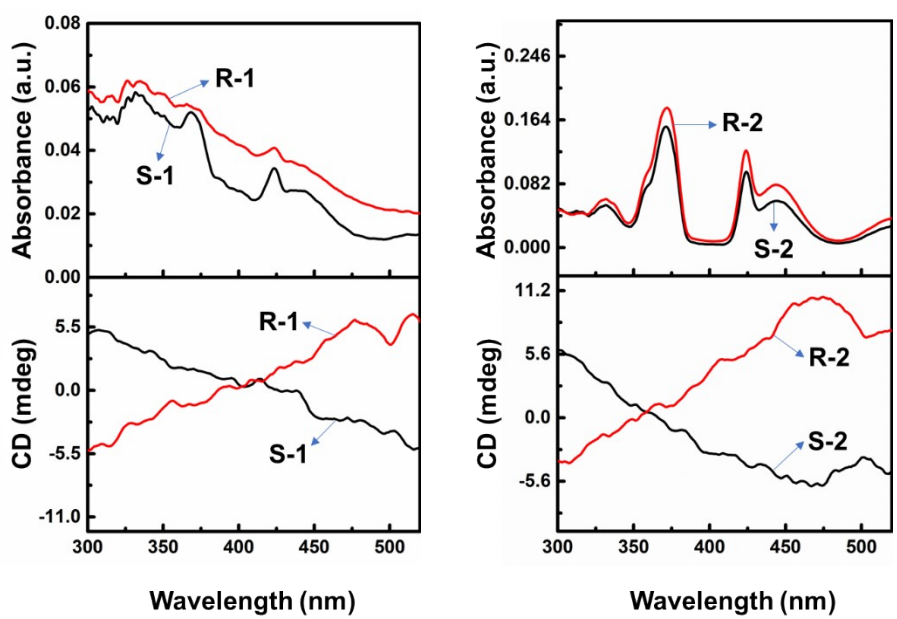


Fig. S6. The CD spectra and UV-Vis absorption spectra of R/S-1 and R/S-2.

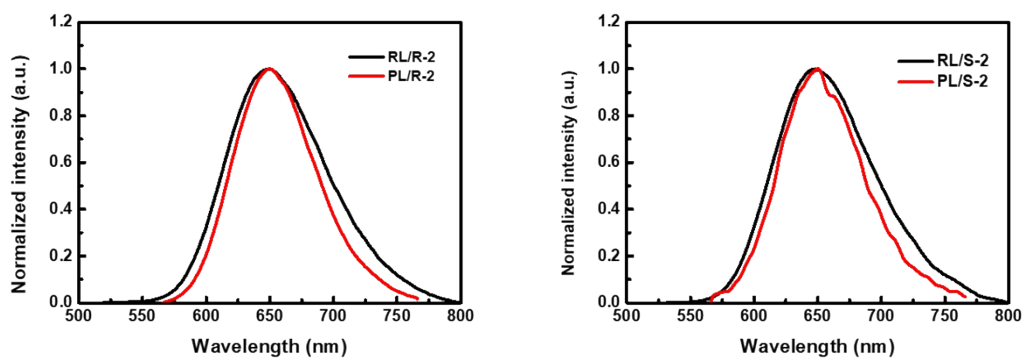


Fig. S7. PL spectra and RL spectra of R/S-1 and R/S-2.

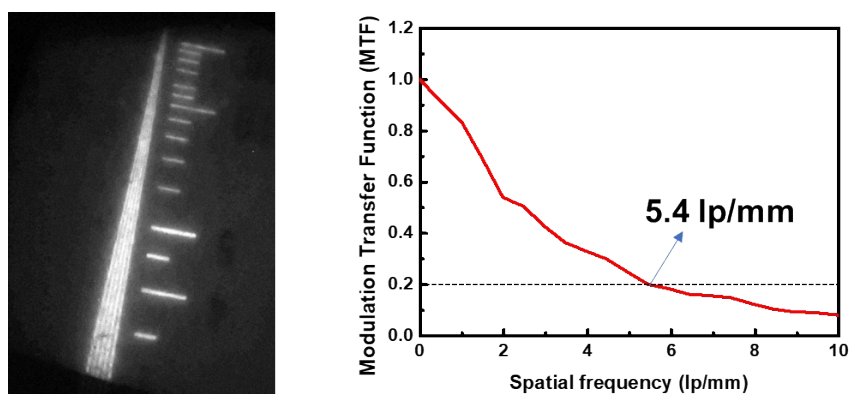


Fig. S8. The standard X-ray test pattern plate and their X-ray images based on R-2

screen (left) and MTF curve extracted from the slanted edge image (right).

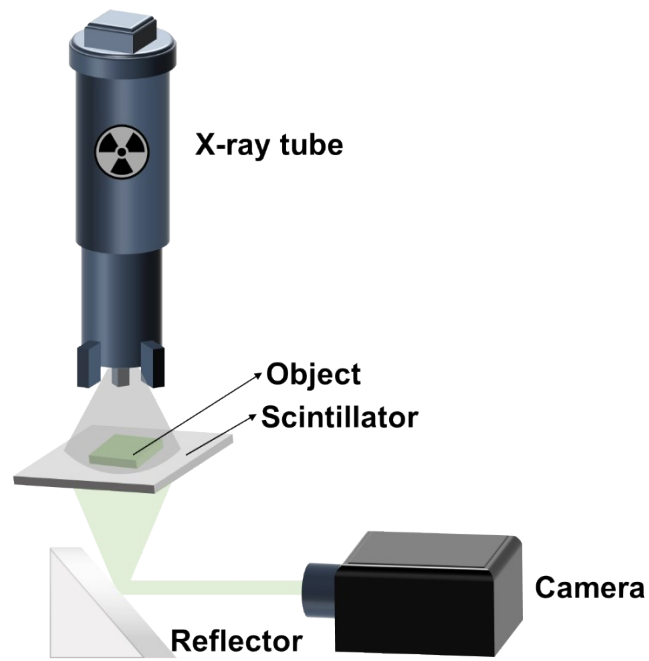


Fig. S9. The spatial distribution diagram of optical imaging system.